The v_3 band of $^{14}C^{16}O_2$ molecule measured by optical-frequency-comb-assisted cavity ring-down spectroscopy

Note: The following files were submitted by the author for peer review, but cannot be converted to PDF. You must view these files (e.g. movies) online.

14CO2_REW.tex

1
2
3
4
5
6
7
8
9
10
11
12
13
14
15
16
17
18
19
20
21
22
23
24
25
26
27
28
29
30
31
32
33
34
35
36
37
38
39
40
41
42
43
44
45
46
47
48
49
50
51
52
53
54
55
56
57
58
59
60

SCHOLARONE™
Manuscripts

For Peer Review Only

RESEARCH ARTICLE

The ν_3 band of ^{14}C^{16}O$_2$ molecule measured by optical-frequency-comb-assisted cavity ring-down spectroscopy

Iacopo Galli^{a,*}, Pablo Cancio Pastor^a, Gianfranco Di Lonardo^b, Luciano Fusina^b,
Giovanni Giusfredi^a, Davide Mazzotti^a, Filippo Tamassia^b, Paolo De Natale^a

^{a}*Istituto Nazionale di Ottica - CNR and LENS, Via N. Carrara 1,*
50019 Sesto Fiorentino FI, Italy
^{b}*Dipartimento di Chimica Fisica ed Inorganica, Università di Bologna,*
Viale del Risorgimento 4, 40136 Bologna, Italy

The infrared spectrum of the rare isotopologue ^{14}C^{16}O$_2$ has been investigated in the range
$2190-2250$ cm^{-1} with a frequency comb-referenced cavity ring-down spectrometer. Thirty-
three ro-vibrational transitions of the ν_3 fundamental band have been detected. Their absolute
frequency was measured with a relative uncertainty ranging from 7.1×10^{-8} to 1.1×10^{-8}. The
experimental frequencies were fitted to the conventional Hamiltonian of a linear molecule and
a new set of spectroscopic parameters for the fundamental vibrational state has been improved
for this species.

Keywords: ^{14}C^{16}O$_2$; infrared spectroscopy; ν_3 fundamental band; optical frequency comb;
cavity ring-down

1.   Introduction

Infrared spectroscopy of radiocarbon dioxide (^{14}C^{16}O$_2$) has been the subject of
very few papers [1–6]. The most recent systematic works on the ν_3 fundamental
band were performed by Sams and De Voe in 1988 [5], and by Dobos *et al.* [6]
in 1989. In Ref. [5], they measured twelve P and R$-$branch transitions by diode
laser spectroscopy. The lines were assigned an uncertainty ranging between 0.001
and 0.005 cm^{-1}. In Ref. [6] a medium resolution (0.18 cm^{-1}) FTIR spectrum and
a high-resolution diode laser spectrum were recorded. In the latter case, the pre-
cision estimated by the authors was better than 0.001 cm^{-1}. Some of the papers
published on this subject dealt with CO$_2$ lasers [3, 4], because the use of ^{14}C^{16}O$_2$
can broaden the working range of spectrometers using CO$_2$ lasers as source of ra-
diation. However, this species is of particular interest for several other reasons. A
spectroscopic study can provide physical information on a still poorly investigated
isotopologue of CO$_2$. This molecule is produced in nuclear power reactors and it is
detected in order to monitor its environmental concentration. This is usually done
through accelerated mass spectrometry [7]. Labrie and Reid [8]showed that radio-
carbon dating can be performed by infrared spectroscopy. Also, ^{14}C measurements
have been carried out on planetary atmospheres [9].

---

*Corresponding author. Email: iacopo.galli@ino.it

In this paper we report on the high-resolution investigation of the fundamental ν_3 band of $^{14}C^{16}O_2$ by comb-referenced cavity ring-down spectroscopy. The main advantages of this technique are: high sensitivity (CO_2 absorptions with line-strength as low as 5×10^{-32} cm can be detected), high resolution (1 kHz) and absolute frequency measurements, which in turn implies that no calibration of the spectra is needed.

2.   Experimental details

Cavity ring-down (CRD) spectroscopy at 4.5 μm was realized to detect thirty-three ro-vibrational transitions belonging to the ν_3 band of $^{14}C^{16}O_2$ molecule. The experimental set-up, described elsewhere [10–12], uses a cw IR coherent radiation at 4.5 μm generated by non-linear frequency difference (DFG) on a periodically-poled MgO:LiNbO$_3$ crystal, placed inside a cw ring Ti:sapphire laser cavity [13]. Such a laser, single-mode operated by optical injection of an external cavity diode laser (ECDL), is the DFG "pump" source, whereas the DFG "signal" light is provided by an external Nd:YAG laser at 1064 nm. A continuous IR tuning between $3850 \div 4540$ nm ($2597 \div 2203$ cm^{-1}) is allowed thanks to the tuning range of the ECDL-Ti:sapphire laser between $834 \div 862$ nm, with a maximum IR power of 25 mW. The IR source is frequency stabilized against an octave-spanning ($500 \div 1100$ nm) fs Ti:sapphire Optical Frequency Comb Synthesizer (OFCS), as "pump" and "signal" frequencies fall within the OFCS spectral operation range [14]. As a consequence, the absolute frequency ν_i of the generated "idler" radiation is given by the following equation:

$$\nu_i = \nu_p - \nu_s = \left(\frac{N_p}{N_s} - 1\right)\nu_s + \nu_\mu \tag{1}$$

where N_p and N_s are the integer orders of the closest comb modes to the "pump" and "signal" absolute frequencies, ν_p and ν_s respectively. As the Nd:YAG laser frequency drift is controlled against the nearest OFCS mode, the absolute frequency of the IR radiation is stable to about 6×10^{-13} at 1 s and accurate to 10^{-12}, both limited by the performance of the Rb/GPS-disciplined 10-MHz quartz reference oscillator of our OFCS. In addition, synthesized IR frequency scans with a Cs-frequency standard traceability can be performed by changing the microwave synthesizer frequency ν_μ in Eq. 1. With this procedure a maximum scan of 450 MHz (a bit less than half the repetition rate of the OFCS) can be performed, wide enough to detect the whole absorption line profiles of the observed transitions for the molecular gas conditions of the present measurements. The generated "idler" IR radiation, sent out of the Ti:sapphire cavity thanks to dispersion at the λ_p-Brewster-cut output facet of the non-linear crystal, is efficiently coupled into a 1-m-long high-finesse ($F \approx 11600$) Fabry-Perot cavity (FPC) for CRD spectroscopy. When the FPC is loaded up to a threshold level, the IR light is quickly switched off-resonance by using an AOM placed on the Nd:YAG laser, and transmitted photons leaking out of the cavity are detected by a InSb photodiode. The CRD decay signal is acquired by a 18-bit digitizing oscilloscope with a sampling rate of 10 MS/s. The measured decay time, $\tau_c = 1/\gamma_c$ for empty-cavity conditions is about 12 μs ($\gamma_c \approx 86$ ms^{-1}).

Such a set-up is suitable for linear-absorption CRD spectroscopy [15] and saturated-absorption cavity ring-down (SCAR) spectroscopy [10], with sensitivity figures, expressed in terms of the minimum detectable absorption coefficient α_{min}, of 10^{-9} and 10^{-10} cm^{-1}Hz$^{-1/2}$, respectively. Although line-strengths of the ro-vibrational transitions of $^{14}C^{16}O_2$ ν_3 band are expected to be of the same order

of magnitude as other CO_2 isotopologues (about 10^{-18} cm for the most intense), the very low natural abundance of such species ($\approx 10^{-12}$) needs high-sensitivity spectroscopy techniques, as CRD, to be detected. For the measurements presented here a pure $^{14}C^{16}O_2$ sample would be preferred, to get the highest possible signal without absorption interferences from other CO_2 lines. Unfortunately, it is very difficult to handle such a sample, taking into account also radioactivity safety reasons. Only spectroscopy of a few orders of magnitude ^{14}C-enriched samples (with respect to natural abundance) is feasible, which has partly prevented the spectroscopic measurements of such molecule. Even in these enriched samples, ultra-sensitive techniques such as CRD or SCAR are required. As a price to pay, other CO_2 absorptions lying in the same spectral region are also detected, which are added as an interference background to be accurately evaluated (see fitting procedure in the "results and discussion" section for other details). For the measurements presented here, we used a 2200 times ^{14}C-enriched CO_2 gas. Fig. 1 shows the IR spectra of most part of the ro-vibrational transitions between the P(40) and R(30) lines of $^{14}C^{16}O_2$ ν_3 fundamental band.

Lines from the P(30) to R(30) were recorded by linear-absorption CRD spectroscopy with a total CO_2 pressure of 12 mbar. The FPC was dry-ice cooled in this case to get a gas temperature of 195 K, thus minimizing the interference effects from hot-bands of other CO_2 isotopologues. Nevertheless, strong interferences are detected, as it can be seen in the R-side of Fig. 1.

Lines from the P(40) to P(32) were recorded by SCAR spectroscopy with a total CO_2 pressure of 18 mbar [1]. For these transitions, room temperature (296 K) was used to increase the ground state population, and hence the absorption signal. At the same time, the interfering background is increased, but it is still not larger than the $^{14}C^{16}O_2$ transition to be measured. In addition, the SCAR spectroscopic technique independently measures, in the same decay event, both γ_g and γ_c. The former decay rate $\gamma_g = c\alpha_g$ contains only the saturable part of the gas absorption. The latter includes all other contributions: cavity mirror losses, technical fringes, absorption from non-saturable transitions interfering with the target line.

We plot in Fig. 1 α_g values (left vertical scale) for these SCAR lines, all having a negligible background except P(40), at which frequency the achievable saturation parameter was too low. On the contrary, for the CRD spectra, $\alpha = (\gamma_g + \gamma_c)/c$ was measured (right vertical scale in Fig. 1, where a constant $\alpha_c = 2.87 \times 10^{-6}$ cm^{-1} due to the empty FPC losses was removed), and residual interfering background is present. In fact, the P(10), R(24) and R(28) transitions were not recorded because of the absorbing background.

For all the lines shown in Fig. 1, the acquisition procedure was the same independently of the CRD or SCAR technique used. For each IR absolute frequency, 128 consecutive decay events are averaged, and fitted to the expected CRD or SCAR decay function to obtain as a result α or α_g, respectively. Ten consecutive α (or α_g) values are measured before a $\pm$10-MHz IR frequency step is applied and the FPC length adjusted to retrieve the resonance condition. Each full 400 MHz scan is performed by stepping the frequency once forward (+ sign) and once backward (- sign). After each scan, the α (or α_g) plotted value at each scan frequency is the weighted mean of the 20 measured values (ten + and ten -). This procedure takes about 5 min for each complete scan. In the present gas conditions, linewidths are limited by Gaussian thermal broadening (FWHM 98 MHz and 120 MHz for 195 K and 296 K respectively) and Lorentzian pressure broadening [16]. Hence, a total

---

[1]With respect to Ref. [10], valid in the inhomogeneous broadening regime, the theoretical model to fit the SCAR signals was adjusted to work at these pressure conditions [12].

400 MHz scan is adequate to record a whole line profile. We note finally that in Fig. 1 all spectra were arranged together, one close to the other in a relative frequency scale, for the sake of clarity. For the analyzed spectra, the frequency scale is absolute and reproducible against the OFCS, as described above.

3. Results and Discussion

Only thirty-three transitions, plotted in Fig. 1, were detected in our experiments. The main limitations to the detection of transitions with higher values of J arose from the operating frequency range of the spectrometer, the weakness of the high$-J$ transitions, even at room temperature, as well as the overlap with lines of more abundant isotopologues. The central frequency of each transition was measured by fitting the line profile to the expected Voigt profile, plus absorbing background. The fit residuals, both for CRD and SCAR measurements, are flat within noise, with no evidence of collisional narrowing [17]. Initial parameters for frequencies and intensities of the interfering transitions were obtained from the HITRAN database [16]. Unfortunately, the uncertainty of these data, if compared with the frequency precision and sensitivity of our measurements, and the presence of CO_2 transitions not listed by the database made difficult, and sometimes impossible, to evaluate the absorbing background. This effect is more important for CRD spectra, and the P(22), P(16), R(0) and R(10) transitions are an example of that; in addition, background due to technical fringes was also considered. For the Voigt profile of the $^{14}C^{16}O_2$ transitions, Gaussian linewidth was always fixed to the required value by each temperature condition. The other line parameters, area, Lorentzian linewidth, and center frequency were left free. In Fig. 1, the agreement between experimental data and fit function (solid line trace) is evident in both CRD and SCAR experimental methodologies.

For each transition, several fit attempts were done with different absorbing background parameters, either fixing or not the Lorentzian linewidth, in order to get the influence of such change in the final line center uncertainty. We have also checked for possible systematic errors due to use of two different recording methods (CRD and SCAR spectroscopy) by using the P(26) transition as a trial test. The good agreement between different recordings is evident in Fig. 1, where this line is plotted in the two cases. In particular, the P(26) measured by CRD is affected only by technical fringes and background offset (no interfering lines), while the SCAR measurement exhibits no background at all. It is worth noting that this is one of the main advantages intrinsic to the SCAR technique. The different spectral areas are simply due to different temperature conditions. The results, including final standard errors are listed in Table 1. The line center uncertainty from the fit is several times lower (one order of magnitude for some transitions) than the final error reported in Table 1. However, we believe that the background parameters' uncertainties derived from the line profile fits were underestimated. We thought that a more realistic approach was to correct the fits uncertainties by individual factors, based on the goodness of the profile and the influence of contributions such as overlaps with other transitions and interference fringes.

Systematic corrections and uncertainties were considered in the transition frequencies reported in Table 1. Concerning the pressure shift, there are no literature data for transitions of this molecule, and we considered the contribution to be equal to that of the transitions of the ν_3 band of $^{13}C^{16}O_2$ [16]. In addition, we did not consider the J dependence of such shift, but we preferred to apply a more conservative procedure. A mean pressure shift correction value was applied for all measured transitions, as a result of the average of the tabulated values for the correspond-

ing transitions of $^{13}C^{16}O_2$. The uncertainties of these corrections are given by the standard deviation of such averages and it was added to the estimated line center fit error. As a result, the CRD measurements were blue-shifted by 0.9 MHz and their uncertainty increased by 0.5 MHz, while the SCAR measurements were blue-shifted by 1.3 MHz and their uncertainty increased by 0.7 MHz. Finally, frequency calibration was not required, thanks to the primary Cs-standard traceability of our measurements. Also, the uncertainty due to the OFCS accuracy was not considered because, even in the worst case (67 Hz for R(30) transition), it is negligible with respect to other contributions.

This ν_3 fundamental infrared band of CO_2 is a $\Sigma - \Sigma$ parallel band with the usual P− and R−branch structure and lacking a Q−branch. The data were analysed using the basic Hamiltonian of a linear molecule, with centrifugal distortion corrections up to the quartic term for the ground state and to the octic term for the upper vibrational state. The ro-vibrational energy term values for non-degenerate vibrational modes of a linear molecule are given by

$$T(v,J) = G_v + B_v J(J+1) - D_v[J(J+1)]^2 + H_v[J(J+1)]^3 + L_v[J(J+1)]^4 \quad (2)$$

The band centre is defined as

$$\nu_0 = G_{v'} - G_{v''} \quad (3)$$

where $G_{v'}$ and $G_{v''}$ represent the purely vibrational energy of the upper and lower state, respectively. The parameters for the upper state $v_3 = 1$, B_1, D_1, H_1 and L_1, were held fixed at the very accurate values of Ref. [4] while the ground state constants B_0 and D_0 were fitted, together with the band centre ν_0. The results of the fit are shown in Table 2. In the fitting procedure the lines were given a weight according to the uncertainties reported in Table 1. The tolerance for rejection was chosen line by line and fixed at twice the standard error associated to the lines. Only four lines were rejected from the fit.

The parameters obtained from the fit are well determined and are considerably improved in terms of both accuracy and precision with respect to the best constants available in literature [6]. The great precision obtained in this work for the band centre, together with the very precise constants of Ref. [4] allowed the determination of the vibrational energy of the levels of the Fermi dyad involved in the CO_2 laser excitation mechanism. In Ref. [4], they reported $\nu(001 - I) = 2.5965917618(13) \times 10^7$ MHz and $\nu(001 - II) = 2.94600023911(49) \times 10^7$ MHz. We eventually derived $\nu(I) = 4.076192962(51) \times 10^7$ MHz and $\nu(I) = 3.726784485(51) \times 10^7$ MHz.

4.   Conclusions

The detection of the ν_3 fundamental band of $^{14}C^{16}O_2$ has been performed with a OFCS-referenced cavity ring-down spectrometer. Several ro−vibrational transitions ranging from P(40) to R(30) have been detected and analyzed. The band origin ν_0 and the ground state parameters B_0 and D_0 have been determined with accuracy improved by about one order of magnitude. This experiment shows the potential of this technique in terms of accuracy and sensitivity and provides important information on a rare isotopologue of CO_2.

6   *I. Galli* et al.

Acknowledgements

References

[1] M. Wahlen, R. S. Eng and K. W. Nill, Appl. Opt. **16**, 2350 (1977).

[2] R. S. Eng, K. W. Nill and M. wahlen, Appl. Opt. **16**, 3072 (1977).

[3] C. Freed, L. C. Bradley and R. G. O'Donnell, IEEE J. Quantum Electron. **16**, 1195 (1980).

[4] L. C. Bradley, K. L. Soohoo and C. Freed, IEEE J. Quantum Electron. **22**, 234 (1986).

[5] R. L. Sams and J. R. DeVoe, J. Mol. Spectrosc. **128**, 296 (1988).

[6] S. Dobos, G. Winnewisser, F. Kling and J. Mink Z. Naturforsch. A **44**, 633 (1989).

[7] C. Melazo Dias, K. Stenström, I. L. Bacelar Lëao, R. Ventura Santos, I. Gomes Nícoli, G. Skog, P. Ekström, R. da Silveira Corrêa and J. Environ. Radioact. **100**, 574 (2009).

[8] D. Labrie and J. Reid, Appl. Phys. A **24**, 381 (1981).

[9] B. M. Jakosky, R. C. Reedy and J. Masarik, J. Geophys. Research **101**, 2247 (1996).

[10] G. Giusfredi, S. Bartalini, S. Borri, P. Cancio, I. Galli, D. Mazzotti and P. De Natale, Phys. Rev. Lett. **104**, 110801 (2010).

[11] P. Cancio, S. Bartalini, S. Borri, I. Galli, G. Gagliardi, G. Giusfredi, P. Maddaloni, P. Malara, D. Mazzotti and P. De Natale, Appl. Phys. B **102**, 255 (2011)

[12] I. Galli, S. Bartalini, S. Borri, P. Cancio, D. Mazzotti, P. De Natale and G. Giusfredi, *Molecular gas sensing down to parts per quadrillion: Radiocarbon-dioxide optical detection* (2011), submitted to Phys. Rev. Lett.

[13] I. Galli, S. Bartalini, S. Borri, P. Cancio, G. Giusfredi, D. Mazzotti and P. De Natale, Opt. Lett. **35**, 3616 (2010).

[14] I. Galli, S. Bartalini, P. Cancio, G. Giusfredi, D. Mazzotti and P. De Natale, Opt. Express **17**, 9582 (2009).

[15] D. Mazzotti, P. Cancio, A. Castrillo, I. Galli, G. Giusfredi and P. De Natale, J. Opt. A **8**, S490 (2006).

[16] L. S. Rothman, I. E. Gordon, A. Barbe, D. C. Benner, P. F. Bernath, M. Birk, V. Boudon, L. R. Brown, A. Campargue, J.-P. Champion, K. Chance, L. H. Coudert, V. Dana, V. M. Devi, S. Fally, J.-M. Flaud, R. R. Gamache, A. Goldman, D. Jacquemart, I. Kleiner, N. Lacome, W. J. Lafferty, J.-Y. Mandin, S. T. Massie, S. N. Mikhailenko, C. E. Miller, N. Moazzen-Ahmadi, O. V. Naumenko, A. V. Nikitin, J. Orphal, V. I. Perevalov, A. Perrin, A. Predoi-Cross, C. P. Rinsland, M. Rotger, M. Simeckova, M. A. H. Smith, K. Sung, S. A. Tashkun, J. Tennyson, R. A. Toth, A. C. Vandaele and J. Vander Auwera, J. Quant. Spectrosc. Radiat. Transfer **110**, 533 (2009).

[17] P. L. Varghese and R. K. Hanson, Appl. Opt. **23**, 2376 (1984).

The ν_3 band of $^{14}C^{16}O_2$ molecule   7

Table 1. Transitions frequencies, uncertainties and residuals from the fit of the lines measured for the ν_3 fundamental band of $^{14}C^{16}O_2$. All numbers are in MHz.

Transition	Obs. Freq.	Uncertainty[a]	Obs.-Calc.[b]
R(30)	67367614.181	4.795	1.759
R(26)	67294430.381	0.825	2.317∗
R(22)	67218457.563	0.875	0.047
R(20)	67179428.939	0.743	−0.260
R(18)	67139706.163	0.731	−0.314
R(16)	67099289.625	1.017	−0.450
R(14)	67058180.523	0.877	−0.197
R(12)	67016379.675	0.828	0.529
R(8)	66930706.117	1.178	3.834∗
R(6)	66886832.920	1.111	4.442∗
R(4)	66842264.775	1.112	−0.645
R(2)	66797014.526	2.003	0.666
P(2)	66680873.788	2.765	−3.952
P(4)	66633216.481	3.176	−5.929
P(6)	66584878.904	1.132	−3.113∗
P(8)	66535859.047	1.443	1.710
P(12)	66435758.242	0.996	−0.005
P(14)	66384685.331	2.458	−0.078
P(18)	66280498.427	0.801	1.310
P(20)	66227383.132	0.865	−0.128
P(24)	66119121.905	1.715	1.758
P(26)	66063972.706	0.755	0.194
P(28)	66008145.242	1.749	−3.339
P(32)	65894474.448	0.747	−0.680
P(34)	65836627.418	0.742	0.147
P(36)	65778106.638	0.729	0.186
P(38)	65718914.039	0.752	0.510
P(40)	65659047.695	1.795	−1.677

[a] See text for a discussion about the uncertainty of the lines.

[b] Lines marked with an asterisk exceeded the tolerance for rejection and were excluded from the fit.

8   *I. Galli* et al.

Table 2. Spectroscopic parameters (in cm^{-1}) obtained for the ν_3 fundamental band of $^{14}C^{16}O_2$.

Parameter	This work[a]	Ref. [6]
ν_0	2225.801399(17)	2225.80239(16)
B_0	0.390253082(58)	0.39025488(18)
$D_0 \times 10^{-7}$	1.33144(37)	1.3372(20)
B_1	0.38739025628[b]	
$D_1 \times 10^{-7}$	1.327523[b]	
$H_1 \times 10^{-14}$	-3.08[b]	
$L_1 \times 10^{-17}$	1.244[b]	
$\sigma_{FIT} \times 10^{-5}$	3.1	

[a] The quantity in parentheses is one standard deviation in units of the last quoted digit.
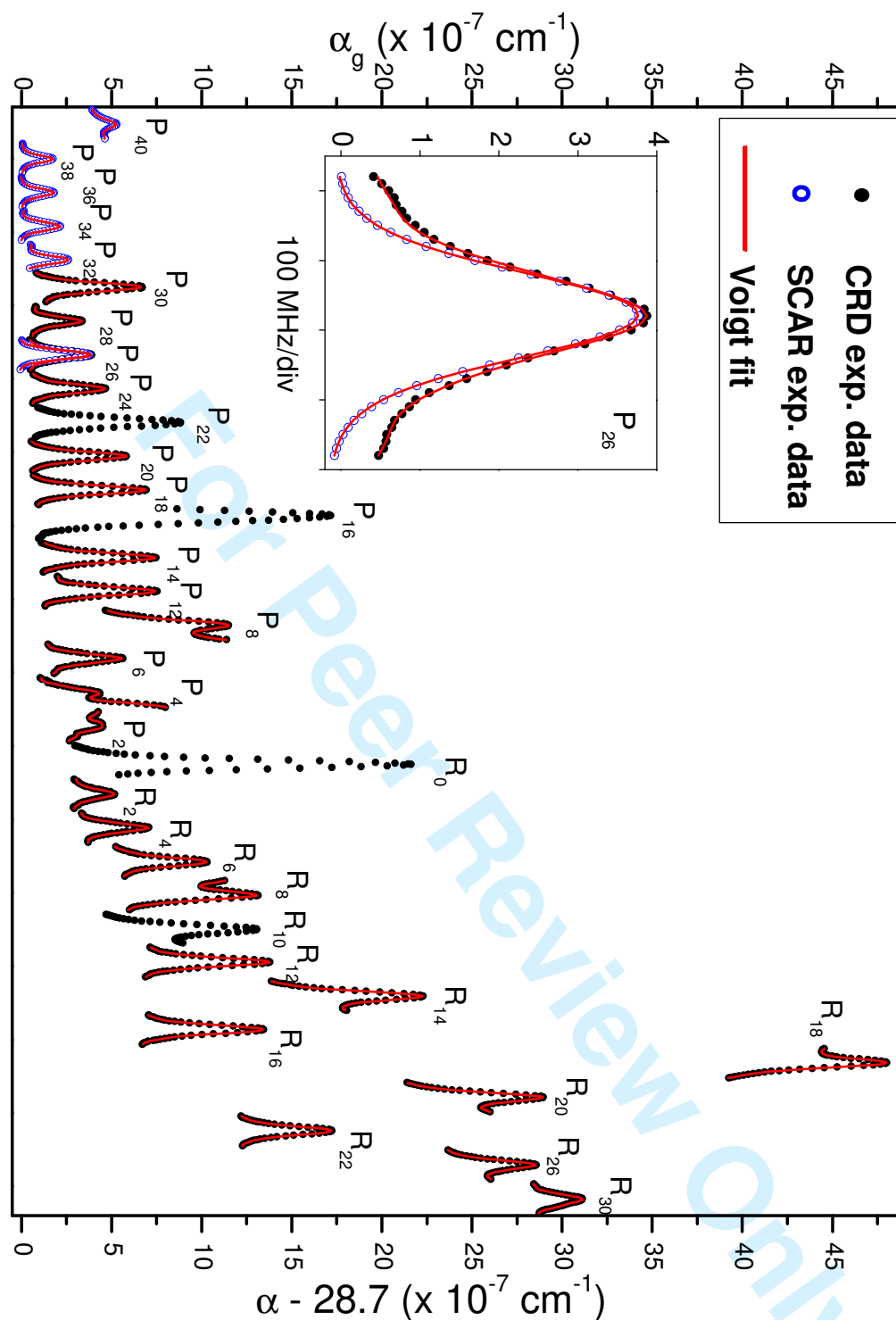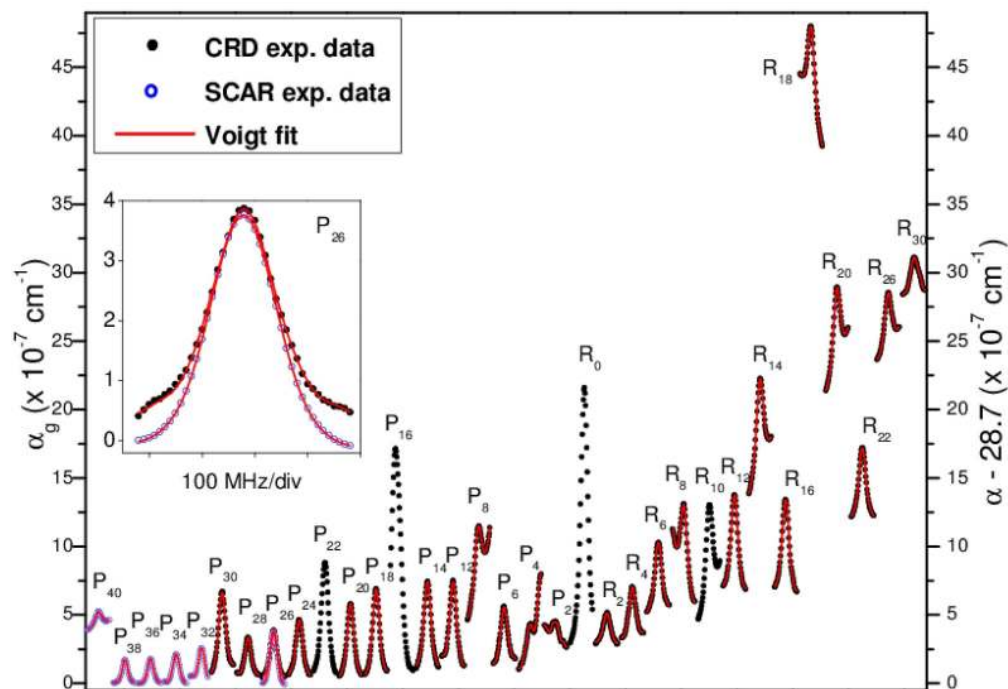
[b] Fixed at the values of Ref. [4]

Figure 1. Overview of the infrared spectrum of $^{14}C^{16}O_2$ molecule in the ν_3 band region. P(40)-P(32) lines were recorded by SCAR spectroscopy, while P(30)-R(30) lines were recorded by CRD spectroscopy. The fit of all measured transitions to a Voigt profile, that takes into account also the background from other CO_2 lines, is also shown. The spectra are plotted in a relative horizontal frequency scale, and frequency gaps between transitions are not shown for the sake of clarity. The right side vertical scale applies to CRD spectra and the left side vertical scale to SCAR spectra. An empty cavity loss rate of $\alpha_c = 2.87 \times 10^{-6}$ cm^{-1} was removed from the measured rates in the case of CRD spectra to get a comparable scale with the SCAR ones. The CO_2 pressure and temperature are 18 mbar and 296 K for the SCAR spectra, 12 mbar and 195 K for the CRD ones. The acquisition conditions and fit procedure are described in the text.

201x141mm (300 x 300 DPI)